

# Stratified dispersal explains mountain pine beetle's range expansion in Alberta

Evan C. Johnson<sup>1,\*</sup>, Micah Brush<sup>2</sup>, and Mark A. Lewis<sup>2,3</sup>

<sup>1</sup>*Mathematical and Statistical Sciences; University of Alberta; Edmonton, Alberta, Canada*

<sup>2</sup>*Department of Biology; University of Victoria; Victoria, British Columbia, Canada*

<sup>3</sup>*Department of Mathematics and Statistics; University of Victoria; Victoria, British Columbia, Canada*

\* *Corresponding author: Evan Johnson, ecjohns1@ualberta.ca*

# Contents

<b>1</b>	<b>Introduction</b>	<b>4</b>
<b>2</b>	<b>Materials and methods</b>	<b>6</b>
2.1	Background . . . . .	6
2.2	Data . . . . .	6
2.3	Data preparation . . . . .	7
2.4	Model . . . . .	7
2.5	Model validation . . . . .	10
<b>3</b>	<b>Results</b>	<b>10</b>
<b>4</b>	<b>Discussion</b>	<b>14</b>
<b>5</b>	<b>Acknowledgements</b>	<b>18</b>
<b>6</b>	<b>Author contributions</b>	<b>18</b>
<b>7</b>	<b>Data sources</b>	<b>18</b>
<b>A</b>	<b>Robustness check: Study area #2</b>	<b>19</b>
<b>B</b>	<b>Robustness check: inter-annual dispersal variability</b>	<b>21</b>
<b>C</b>	<b>Additional information about characteristic length scales</b>	<b>22</b>
<b>D</b>	<b>Additional figures &amp; tables</b>	<b>26</b>

## Abstract

1. The mountain pine beetle (MPB), a destructive pest native to Western North America, has recently extended its range into Alberta, Canada.
2. Predicting the dispersal of MPB is challenging due to their small size and complex dispersal behavior. Because of these challenges, estimates of MPB's typical dispersal distances have varied widely, ranging from 10 meters to 18 kilometers.
3. Here, we use high-quality data from helicopter and field-crew surveys to parameterize a large number of dispersal kernels.
4. We find that fat-tailed kernels — those which allow for a small number of long-distance dispersal events — consistently provide the best fit to the data. Specifically, the radially-symmetric Student's  $t$ -distribution with parameters  $\nu = 0.012$  and  $\rho = 1.45$  stands out as parsimonious and user-friendly; this model predicts a median dispersal distance of 60 meters, but with the 95<sup>th</sup> percentile of dispersers travelling nearly 5 kilometers.
5. The best-fitting mathematical models have biological interpretations. The Student's  $t$ -distribution, derivable as a mixture of diffusive processes with varying settling times, is consistent with observations that most beetles fly short distances while few travel far; early-emerging beetles fly farther; and larger beetles from larger trees exhibit greater variance in flight distance.
6. Finally, we explain why other studies have found such a wide variation in the length scale in MPB dispersal, and we demonstrate that long-distance dispersal events are critical for modelling MPB range expansion.

**Keywords:** mountain pine beetle, long distance dispersal, stratified dispersal, range expansion, bark beetle, fat-tailed distribution, dispersal kernel

# 1 Introduction

Dispersal is the key factor driving the spread of forest pests. The assumption of simple random motion by individuals leads to a Gaussian distribution for dispersal distances. Although there is tremendous variability in dispersal data, kernels tend to be leptokurtic, having more long and short-distance values than found in a Gaussian distribution with comparable variance (Kot et al., 1996). The spread rate of a biological invasion is critically sensitive to the shape of the dispersal kernel (Lewis et al., 2016). In particular, long-distance dispersal can increase the spread rate by orders of magnitude. In the extreme case of fat-tailed dispersal kernels (those not exponentially bounded like the thin-tailed Gaussian distribution), invasions may continually increase in speed and never achieve a constant spread rate.

The mountain pine beetle (MPB), *Dendroctonus ponderosae* Hopkins (*Coleoptera: Curculionidae*), exemplifies the critical role of dispersal in forest pest invasions. The most recent outbreak of MPB is the largest bark beetle outbreak ever recorded, killing pine trees across western North America and affecting 18 million hectares in British Columbia alone (Taylor et al., 2006b; Walton, 2012). Driven by fire suppression and climate change (Carroll et al., 2006a; Creeden et al., 2014), MPB expanded its historic range in a northeasterly direction, breaching the Rocky Mountains to reach Alberta (Nealis and Cooke, 2014; Carroll et al., 2003; Bleiker, 2019). Although MPB has currently stalled in eastern Alberta (putatively due to some combination of control efforts, host-tree depletion, and unusually cold winters; Janice Cooke qtd. in News, 2023), future outbreaks may invade pine forests stretching to the east coast of North America.

MPB’s recent range expansion into Alberta offers a unique opportunity to study dispersal dynamics due to two key factors: data availability and the absence of endemic populations. MPB uses aggregation pheromones to coordinate mass attacks on pine trees, resulting in rapid drying out of the trees and rust-red foliage. This clear diagnostic feature, along with MPB’s economic importance (Corbett et al., 2016), has led to extensive data collection via aerial surveys. Alberta also lacks endemic populations of MPB, thus eliminating a significant confounding factor. Endemic populations are practically unobservable due to low densities (around 40 individuals per hectare; Carroll et al., 2006b) and because they do not produce the diagnostic red-topped trees; instead of mass-attacking healthy trees, endemic beetles persist in dead or severely weakened trees with a suite of other bark beetles. Therefore, in regions with endemic populations, it is often unclear whether red-topped trees result from endemic beetles becoming able to attack healthy trees (due to climatic conditions or recent disturbances; Bleiker et al., 2014), or from epidemic beetles dispersing from elsewhere.

Describing the flight-based dispersal of MPB is key to describing their spread, yet this task is confounded by biological complexity, as well as our inability to track individual beetles. The dispersal of MPB is influenced by various environmental factors, including wind, temperature, and host-tree availability (Chen and Jackson, 2017; McCambridge, 1971; Powell and Bentz, 2014). At shorter scales, their ability to aggregate and overcome host defenses is facilitated by chemical signaling (Raffa, 2001). Once a tree has been “filled up” with MPB, additional beetles are deterred by anti-aggregation pheromones and auditory signals (i.e. stridulations). More importantly, MPB display distinct dispersal behaviors: they can fly short distances through the forest to find suitable hosts, or they can disperse long distances *en masse* above the canopy, carried by convective wind currents. Both modes of dispersal are important at the landscape scale, but long-distance dispersal events are relatively rare and thus difficult to predict. Existing models of MPB often utilize dispersal kernels (e.g., Gaussian or Laplace distributions) that implicitly ignore long-distance dispersal events, even though these events determine the speed of range expansion (Liu and Kot, 2019).

The existing literature finds significant variation in the typical length scale of MPB dispersal (e.g., the median dispersal distance), from 10 m, to 1 km, to 10s of km (see Table 1). Statistical

models of dispersal — which use covariates like “total infestations within 3 km” rather than dispersal kernels — similarly find that typical dispersal distances vary over several orders of magnitude (e.g., [Preisler et al., 2012](#); [Sambaraju et al., 2012](#); [Powell and Bentz, 2014](#)). This degree of variation cannot be attributed to true spatial or temporal heterogeneity in beetle dispersal. Instead, the wide range of estimates is an artifact of questionable modeling choices (see Discussion).

Table 1: A summary of existing literature on beetle dispersal. We present the study, the characteristic scale of dispersal, and the methodology used. We additionally include the most direct estimates (those from mark-recapture or nearest neighbor studies) for other related bark beetles. Additional information on each of these sources and how we obtained the values in this table are available in Appendix C.

Study	Scale (m)	Method	
<a href="#">Aukema et al. (2008)</a>	18 000	Statistical model	
<a href="#">Koch et al. (2021)</a>	17 000	Dispersal kernel	
<a href="#">Preisler et al. (2012)</a>	10 000	Statistical model	
<a href="#">Sambaraju et al. (2012)</a>	6000	Statistical model	
<a href="#">Howe et al. (2021)</a>	5000	Statistical model	
<a href="#">Carroll et al. (2017)</a>	2000	Nearest neighbor	
<a href="#">Simard et al. (2012)</a>	2000	Statistical model	
<a href="#">Robertson et al. (2009)</a>	1000	Modified nearest neighbor	
<a href="#">Strohm et al. (2013)</a>	364	Other model	
<a href="#">Powell and Bentz (2014)</a>	5 – 90	Other model	
<a href="#">Robertson et al. (2007)</a>	30 – 50	Nearest neighbor	
<a href="#">Safranyik et al. (1992)</a>	30	Mark-recapture	
<a href="#">Heavilin and Powell (2008)</a>	10 – 15	Dispersal kernel	
<a href="#">Goodsman et al. (2016)</a>	10	Dispersal kernel	
Data estimates from related bark beetles			Bark beetle species
<a href="#">Withrow et al. (2013)</a>	1000 – 2500	Nearest neighbor	Douglas-fir beetle
<a href="#">Turchin and Thoeny (1993)</a>	690	Mark-recapture	Southern pine beetle
<a href="#">Werner and Holsten (1997)</a>	90 – 300	Mark-recapture	Spruce beetle
<a href="#">Zumr (1992)</a>	200	Mark-recapture	European spruce beetle
<a href="#">Dodds and Ross (2002)</a>	200	Mark-recapture	Douglas-fir beetle
<a href="#">Kautz et al. (2011)</a>	100	Nearest neighbor	European spruce beetle
<a href="#">Zolubas and Byers (1995)</a>	10	Mark-recapture	European spruce beetle

There have also been attempts to characterize beetle dispersal without an underlying model. A mark-recapture experiment with MPB found typical dispersal distances of around 30 m ([Safranyik et al., 1992](#)), and other mark-recapture experiments with related beetles find similarly short distances (see Table 1). A notable shortcoming of these experiments is that they utilize pheromone traps, which may bias dispersal estimates downwards. Another approach that uses the data directly involves finding new infestations and assigning them to the closest infestation in

the previous year. For brevity, we call these *nearest neighbor studies* in Table 1. Like the mark-recapture studies, nearest-neighbor studies suffer from downward bias, and like the dispersal kernel studies, the nearest-neighbor studies find a large range of typical dispersal distances.

Previous studies do not agree on the scale of MPB dispersal, and it can be difficult to judge individual studies without expertise in both MPB biology and modeling; therefore, there is a need for a reliable, authoritative, and easy-to-use dispersal model. In addition to predicting MPB infestations in the short term, describing MPB dispersal is a key stepping stone to answering longstanding applied questions. These include 1) how spread is affected by host resistance, which is thought to vary both within and across pine species (Cudmore et al., 2010; Six et al., 2018; Srivastava and Carroll, 2023); 2) the relationship between infestation density and dispersal (Safranyik and Carroll, 2006; Jones et al., 2019); 3) the risk of MPB invasion into the low-volume Jack pine stands of Eastern Alberta and Saskatchewan; and 4) the risk of MPB invasion into the high-volume stands of Northwest Ontario (Bleiker, 2019).

In this paper, we parameterize dispersal kernels using high-quality infestation data from the Government of Alberta. The intensive survey effort undertaken provides data on the number of infested trees throughout Alberta with a positional accuracy of  $\pm 30$  m. Importantly, because beetles were not previously present in Alberta, new outbreak locations are not thought to be from erupting endemic beetle populations, but instead from dispersal events. We consider a large class of possible kernels, including thin and fat-tailed distributions. We anticipate that given the importance of long-distance dispersal events in biological invasions, fat-tailed distributions should provide the best fit to the infestation data.

## 2 Materials and methods

### 2.1 Background

Beetles emerge from their natal trees and attack new host trees each summer. If a tree is killed, its foliage will turn rust-red the proceeding summer (or early autumn), approximately one year after the initial attack. Knowing this diagnostic feature of year-old infestations, the Alberta Department of Agriculture and Forestry uses helicopters to find all red-topped trees across vast swaths of Alberta’s forests. These so-called Heli-GPS surveys are an integral part of Alberta’s management strategy for mountain pine beetle. After the heli-GPS surveys are conducted each year (typically around September), field crews are sent to the locations of red-topped trees. The crews then perform concentric ground surveys to find nearby green-attack trees: trees that were recently infested and containing beetle broods. The green-attacked trees are “sanitized” (i.e., burned or chipped) to prevent the proliferation and spread of mountain pine beetle (Government of Alberta, 2016).

### 2.2 Data

Our paper utilizes data from the Alberta Heli-GPS and ground surveys, from 2005–2020. We restricted our main analysis to an approximately 2500 km<sup>2</sup> patch of lodgepole pine forest in western Alberta (Fig. 1). This study area was selected because it contains suitable mountain pine beetle habitat (i.e., high-biomass forest, moderate temperatures), is relatively homogeneous (i.e., low topological complexity, contiguous forest), and was surveyed every year. For robustness, we replicated our analysis on a second 2500 km<sup>2</sup> patch that is approximately 50 km east of the original study area; the results are qualitatively identical, and are thus relegated to Appendix A.

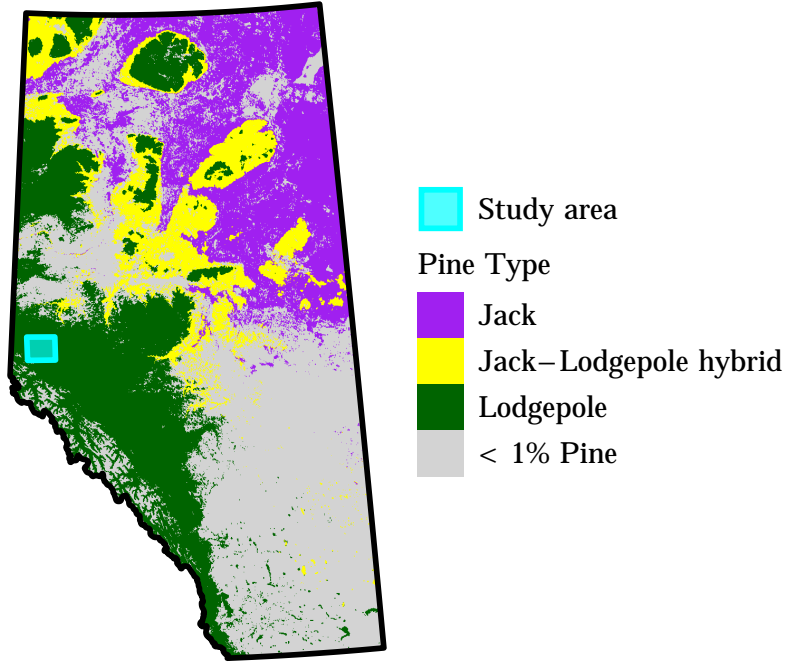


Figure 1: Location of our study area in Alberta. Our study area (cyan) is an approximately 2,500 km<sup>2</sup> block of high-biomass lodgepole pine, and was surveyed annually from 2006–2021. Pine species data comes from [Cullingham et al. \(2012\)](#). The grey pixels are areas where pines constitute less than 1% of total live aboveground biomass; data from [Beaudoin et al. \(2014\)](#).

### 2.3 Data preparation

The raw heli-GPS and ground survey data contain GPS coordinates and the number of trees (red-topped or controlled trees respectively). We rasterized this point data into 30 x 30-meter pixels. Rasterizing with a higher resolution would likely offer no benefits, seeing that location data may have positional errors up to  $\pm 30$  meters.

We use  $I_t(x)$  to denote the number of infested trees in pixel  $x$ , in year  $t$ . The number of infestations is calculated as

$$I_t(x) = c_t(x) + r_{t+1}(x), \quad (1)$$

where  $c_t(x)$  is the number of green-attack trees that were located and “controlled” (i.e., burned or chipped) in the focal year, and  $r_{t+1}(x)$  is the number of red-topped trees observed in the following year. Our overarching goal is to predict the positions of next year’s infestations, given this year’s infestations. However,  $I_t$  is not a suitable model input — it contains green-attack trees that are controlled, and thus cannot contribute to future infestation. Therefore, we define a slightly modified input variable,  $I_t^*(x) = I_t(x) - c_t(x)$ .

### 2.4 Model

Conceptually, our models of mountain pine beetle dispersal are simple (Fig. 2). A dispersal kernel predicts the spatial distribution of infestations in the focal year (*offspring infestations*), stemming from each infestation in the prior year (*parental infestations*). All of these individualized distributions are combined to create a landscape-scale dispersal distribution, and then normalized to create a probability distribution for the offspring infestations. Unlike heuristic methods that calculate distances between offspring infestations and their closest parental source, the model-based approach offers a key advantage by averaging over multiple possible origins for each offspring infestation.

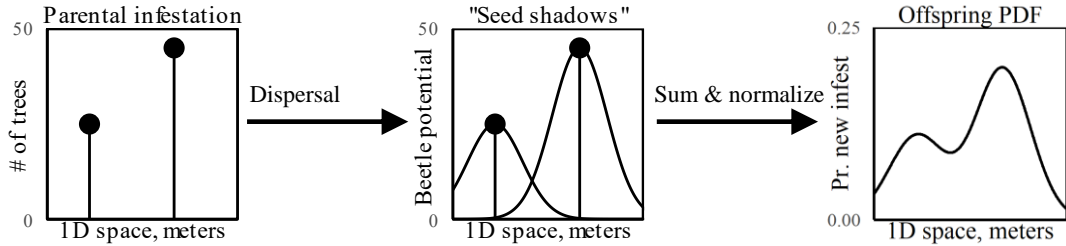


Figure 2: Graphical representation of our redistribution models in one dimension. A dispersal model is applied to each parental infestation, creating surfaces that represent the potential of offspring infestations stemming from parental infestation. These are called “seed shadows” in the plant ecology literature. To create a probability density function for new infestations, we sum and normalize these seed shadows.

We examined a variety of different sub-models for dispersal, summarized in Table 2. The general mathematical form of dispersal kernel is  $D(r = \text{dist}(x, y))$ . The function  $D$  maps the destination coordinate  $y$  and the source coordinate  $x$  to a probability density. Here, each dispersal kernel is assumed to be radially symmetric, and thus each kernel can be parameterized as a function of the Euclidean distance between coordinates,  $r = \text{dist}(x, y)$ . Although we will use the term “dispersal kernel” for its familiarity, the jargon “redistribution kernel” is technically more accurate, since we are not modelling beetle dispersal *per se*, but rather the spatial relationship between infestations.

There are three classes of dispersal kernels: thin-tailed, fat-tailed, and mixtures of thin-tailed distributions. The moniker “thin-tail” describes any distribution whose tails decay exponentially (or faster) in the limit of large  $r$ . The Gaussian distribution is a prime example of this category, exhibiting the fastest decay rate among all the distributions we examined. By contrast, fat-tailed distributions decay slower than exponentially. The Pareto distribution is a prime example of this category, with tails so fat the variance of the distribution doesn’t exist when the scale parameter  $\nu < 2$ . Mixture distributions, which are weighted averages of two thin-tailed distributions, technically remain thin-tailed due to their asymptotic behavior, but can simulate fat-tailed distributions over intermediate distances by blending distributions with various distance scales. The flexible nature of mixtures is illustrated by the radially symmetric Student’s  $t$ -distribution, also referred to as the “2Dt dispersal kernel”. This properly fat-tailed distribution can be derived as an infinite mixture of Gaussian distributions whose variances are prescribed to follow an inverse-gamma-distribution (Lewis et al., 2016).



Table 2: All of the dispersal kernels that were fit to the Alberta Heli-GPS data, along with their tail-type classification, functional form, and mechanistic interpretation. The Whittle–Matérn–Yasuda kernel (abbr. WMY) contains the function  $K_\kappa$  denoting the  $\kappa^{\text{th}}$  order modified Bessel function of the second kind. The parameter  $\nu$  is constrained to be greater than 1; otherwise, the normalizing constant of the distribution does not exist. This table was inspired by Table 1 in Koch et al. (2020).

Kernel name	Tail type	$D(r) \propto$	Mechanistic derivation
Pareto	Fat	$(r + \rho)^{-(1+\nu)}$	Levy random walk; successive dispersal steps from a mixture of distributions with disparate characteristic length scales (Benhamou, 2007)
Student's $t$	Fat	$\left(1 + \frac{1}{\nu} \left(\frac{r}{\rho}\right)^2\right)^{-\frac{\nu+1}{2}}$	2D Fickian diffusion with inverse-gamma-distributed settling times (Lewis et al., 2016, pg. 167)
Bessel mixture	Mixture of Thin	$\theta K_0\left(\frac{r}{\rho_1}\right) + (1 - \theta)K_0\left(\frac{r}{\rho_2}\right)$	2D Fickian diffusion with two different motilities and/or two different settling rates.
Laplace mixture	Mixture of Thin	$\theta \exp\left(-\frac{r}{\rho_1}\right) + (1 - \theta) \exp\left(-\frac{r}{\rho_2}\right)$	2D Fickian diffusion with two different motilities and instantaneous settling.
Gaussian mixture	Mixture of Thin	$\theta \exp\left(-\left(\frac{r}{\rho_1}\right)^2\right) + (1 - \theta) \exp\left(-\left(\frac{r}{\rho_2}\right)^2\right)$	2D Fickian diffusion with two different motilities and a single settling time, or a single motility constant and two different settling times.
WMY	Thin	$\left(\frac{r}{\rho}\right)^\kappa K_\kappa\left(\frac{r}{\rho}\right)$	2D Fickian diffusion with gamma-distributed stopping times or 2D fractal diffusion with constant settling rate (Koch et al., 2020)
Bessel	Thin	$K_0\left(\frac{r}{\rho}\right)$	2D Fickian diffusion with constant settling rate (Broadbent and Kendall, 1953)
Laplace	Thin	$\exp\left(-\frac{r}{\rho}\right)$	Turbulent diffusion then instantaneous settling (Joseph and Sendner, 1958) or a bout of 2D Fickian diffusion followed by a bout of fractal diffusion, then instantaneous settling (Koch et al., 2020)
Gaussian	Thin	$\exp\left(-\left(\frac{r}{\rho}\right)^2\right)$	2D Fickian diffusion then instantaneous settling (Skellam, 1951)

The likelihood function is computed by first convolving the map of the parental infestations,  $I_{t-1}^*(x)$ , with the dispersal kernel:

$$B_t(y) = \sum_x I_{t-1}^*(x) D(\text{dist}(y, x)) (\Delta x)^2, \quad (2)$$

with  $\Delta x = 0.03\text{km}$  as the spatial resolution. The result is the *beetle potential*  $B_t$ , which represents the average number of beetles arriving at each location. Note that Eq. 2 is the discretization of a continuous-space convolution; thus,  $\text{dist}(y, x)$  is the distance between the centers of two 30-meter pixels, regardless of the spatial distribution of infestations within those pixels.

The beetle potential is re-scaled to produce a likelihood surface:

$$\pi_t(x) = \frac{B_t(x)}{\sum_y I_{t-1}^*(y)} \quad (3)$$

While the convolution is performed for all infestations within the approximately 50x50 km study area, the likelihood is only calculated using the new infestations that were further than 10km from the boundary of the study area. This buffer zone circumvents statistical edge effects, ensuring that each modeled infestation is allowed to receive virtual beetles from all directions. Each offspring infestation is treated as an i.i.d. event, and thus the log likelihood in year  $t$  is

$$\mathcal{L}_t = \sum_{x: I_t(x) > 0} I_t(x) \times \log(\pi_t(x)). \quad (4)$$

The total log likelihood is simply the sum over years, from 2009 to 2019:  $\mathcal{L} = \sum_{t=1}^{11} \mathcal{L}_t$ . While the presence of MPB in Alberta dates back to 2005, the years 2009–2019 constitute the main phase of heightened MPB presence (Fig. D.1).

All dispersal kernels were fit with maximum likelihood estimation. More specifically, multi-parameter kernels were fit with the Nelder-Mead algorithm, whereas the single-parameter kernels (i.e. the Laplace, Gaussian, and Bessel) were optimized using high-resolution likelihood profiles (Fig. D.2). All analyses were performed in R (Team, 2022)

## 2.5 Model validation

The dispersal models were validated and compared using a holistic approach that combined metrics of relative model fit (e.g. the log likelihood), absolute model fit (e.g. forecast correlation, true detection rate), and the visual agreement between model predictions and salient features of the data. Notably, we calculated the distance between offspring infestations and the nearest parental infestation. This nearest neighbor analysis produces a lower bound for model-based estimates of dispersal distance, indicates the general shape of the marginal dispersal kernel, and helps us roughly classify observations as short or long-distance dispersal events. This classification enables us to assess models more effectively by examining the log likelihood of observations within defined categories of dispersal distance.

To explore the long-term implications of the different dispersal kernels, we simulated the spread of MPB across Alberta. Each simulation started with the same initial conditions, the observed infestations in 2005. Then, for each successive year, the simulated infestations determine the beetle-potential surface and corresponding probability mass function, from which the new infestations are simulated. The number of simulated infestations is equal to the actual number of observed infestations in the focal year; this methodology accounts for the fact that some years (particularly the 2008–2009 transition) exhibit variable reproductive rates, potentially because of fluctuating climatic factors. The simulation was constrained to areas where lodgepole pine is the dominant pine species and where pine biomass constitutes more than 1% of total live aboveground biomass.

## 3 Results

Across all forms of evidence, the most effective models featured fat-tailed dispersal kernels. There were larger differences between the three categories of dispersal kernels — thin-tailed, fat-tailed, and mixture — than there were within each category (Fig. 3, leftmost panel). The differences between fat-tailed and mixture-based dispersal kernels are subtle, whereas models with thin-tailed dispersal kernels consistently performed worse by all measures of quality.

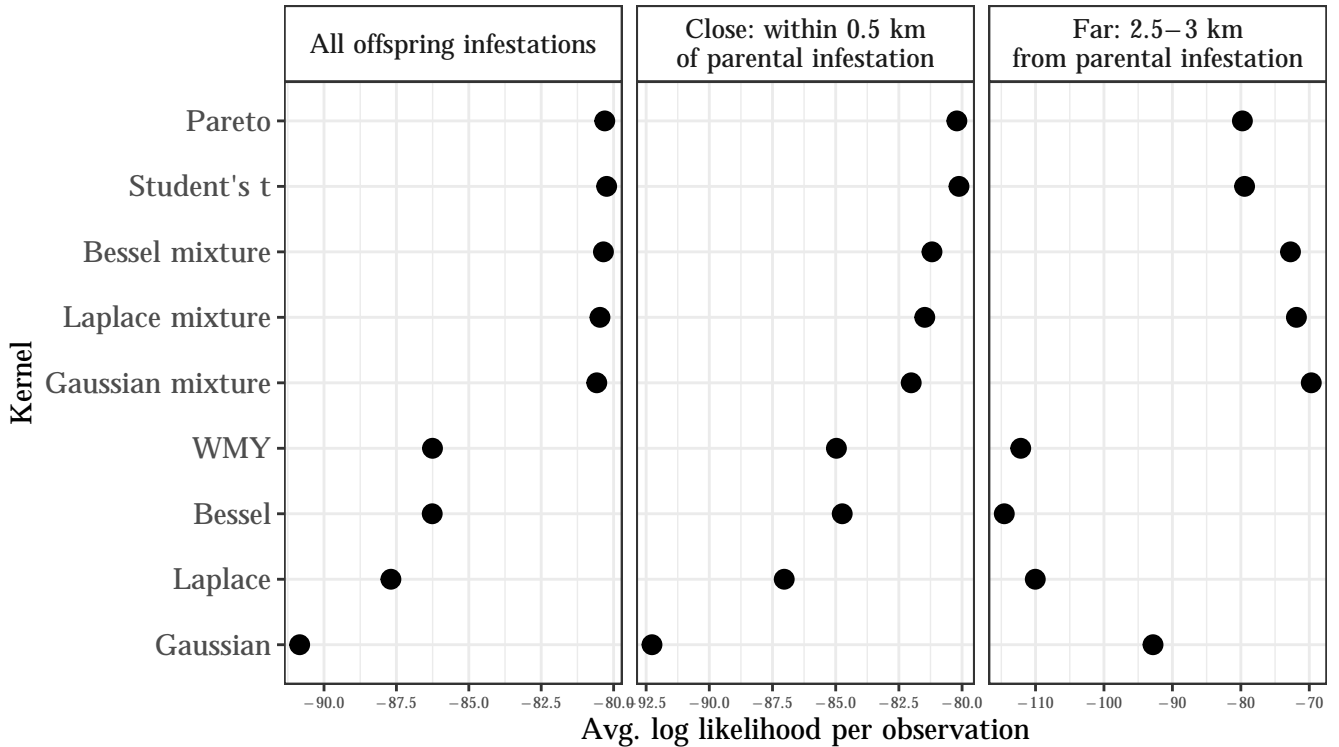


Figure 3: Model fit for observations that are various distances from the nearest parental infestations. Observations that were within 0.5 kilometers of the nearest parental infestation (representing short-to-medium distance dispersal) were best modeled by the fat-tailed distributions, the Pareto and Student’s  $t$ -distributions. Observations that were within 2.5–3 km from the nearest parental observation were best modeled by the mixture distributions.

Thin-tailed dispersal kernels, like the familiar Gaussian and Laplace kernels, consistently produced low log likelihoods, predictive correlations, and true positive rates for new infestations (Table 3). There is a huge log likelihood penalty for dispersal kernels that predict a near-zero infestation probability for a pixel in which an infestation does occur; to avoid this penalty, the thin-tailed dispersal kernels predict that most dispersal is medium-distance dispersal. This phenomenon is most evident in the case of the Gaussian dispersal kernel, which has the fastest-decaying tails of any distribution considered here, and consequently predicts a median dispersal distance of 1.1 km (Table 3). This is probably wrong, since the majority of experiments and models — including our other dispersal kernels — imply that most beetles disperse much shorter distances. The general pattern, wherein thin-tailed kernels predict a predominance of medium-distance dispersal, is readily visualized with a 2D log-likelihood surface (Fig. 4).

Table 3: Summary statistics of model fit and redistribution distances for the redistribution models, fit to data from study area #1. The abbreviation TPR stands for *True Positive Rate*;  $r$  is the correlation between the logarithm of the observed number of infestations and the logarithm of the expected number of infestations; and the last 4 columns refer to the distances between new infestations and their parental infestations. To compute the TPR, we identify a “positive” as one or more infestations within a 30 x 30-meter pixel, and we predict a positive when the probability of one or more infestations is greater than 1/2. This probability is computed as the complement of the Bernoulli probability of observing zero new infestations, given a number of trials equal to the total infestations observed in the focal year, and the per trial probability is derived from the redistribution model. The expected number of infestations (used in the calculation of  $r$ ) is simply the per-trial probability of an infestation, multiplied by the total number of infestations in the focal year.

Kernel name	Log likelihood	TPR	$r$ (log scale)	mean dist.	median dist.	75% dist.	95% dist.
Pareto	$-7.494 \cdot 10^5$	0.009	0.327	0.957	0.080	0.320	3.950
Student's $t$	$-7.488 \cdot 10^5$	0.015	0.330	1.059	0.060	0.270	4.670
Bessel mixture	$-7.498 \cdot 10^5$	0.004	0.343	2.571	0.070	3.440	12.940
Laplace mixture	$-7.510 \cdot 10^5$	0.004	0.346	3.043	0.070	4.850	13.920
Gaussian mixture	$-7.520 \cdot 10^5$	0.013	0.348	4.695	1.730	8.730	15.690
WMY	$-8.049 \cdot 10^5$	0.000	0.170	0.355	0.280	0.480	0.900
Bessel	$-8.050 \cdot 10^5$	0.000	0.168	0.338	0.270	0.460	0.860
Laplace	$-8.183 \cdot 10^5$	0.000	0.148	0.429	0.360	0.580	1.020
Gaussian	$-8.477 \cdot 10^5$	0.000	0.096	0.982	0.920	1.300	1.920

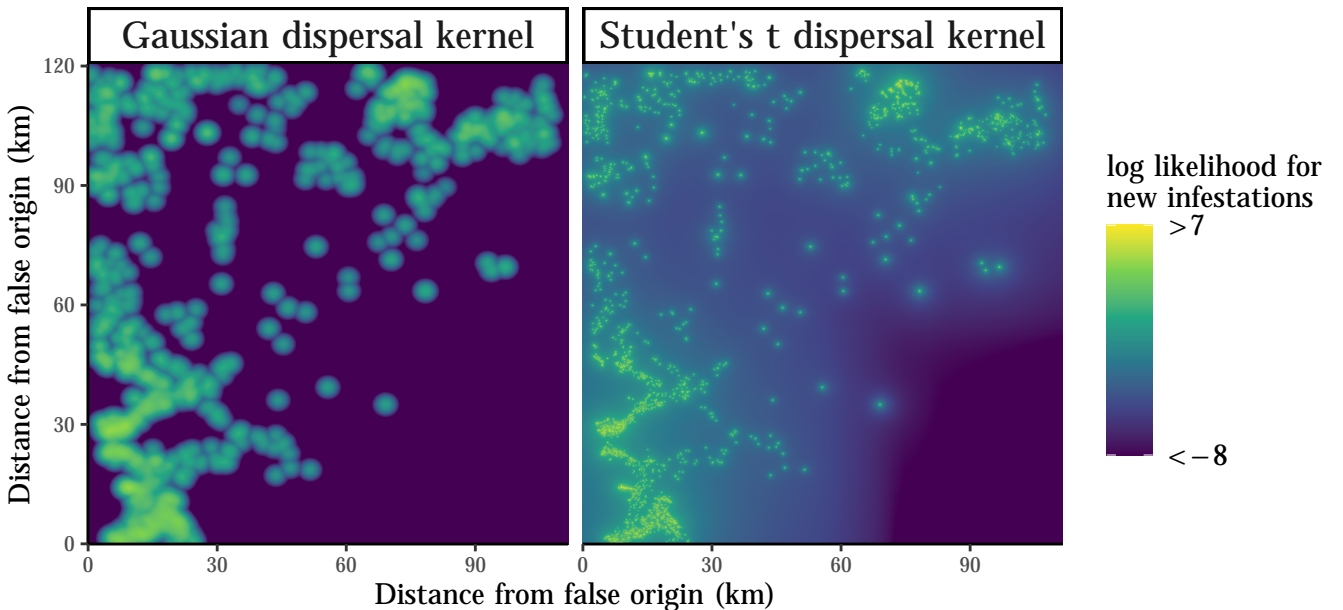


Figure 4: In order to account for medium-to-long distance dispersal events, thin-tailed redistribution kernels (here, the radially-symmetric Gaussian) predict that offspring infestations will be several kilometers from parental infestations. The fat-tailed dispersal kernels (here, the radially-symmetric Student's  $t$ ) predominantly predict short-distance dispersal, along with a small number of long-distance dispersal events. The maps display model predictions of beetle potential from trees that were infested in 2006. The origin has coordinates longitude & latitude coordinates -119.7269,53.60261.

Fat-tailed kernels produce higher log likelihoods than mixture-based kernels, but the difference is slight, thus suggesting that the two types of dispersal kernels be differentiated based on

additional features. Both predict a majority of short-distance dispersal and a minority of long-distance dispersal, but the mixture models are more extreme. To see this, consider the Laplace kernel with density  $\exp(-r/\rho)$ , which has the nice property of the mean distance equaling  $2 \times \rho$  km. The Laplace mixture model predicts that a  $\theta = 0.62$  proportion of beetles engage in short-distance dispersal with a mean distance of 42 meters, while the remaining beetles disperse with a mean distance of 7.8 km (Table 4).

Table 4: Parameter values for the redistribution models, fit to data from study area #1. The parameters  $\rho$ ,  $\rho_1$ , and  $\rho_2$  have units of kilometers; the remaining parameters are dimensionless.

Kernel name	Tail type	$D(r) \propto$	Max likelihood estimate
Pareto	Fat-tail	$(r + \rho)^{-(1+\nu)}$	$\rho = 1.35 \cdot 10^{-2}$ , $\nu = 1.57$
Student's $t$	Fat-tail	$\left(1 + \frac{1}{\nu} \left(\frac{r}{\rho}\right)^2\right)^{-\frac{\nu+1}{2}}$	$\rho = 1.18 \cdot 10^{-2}$ , $\nu = 1.45$
Bessel mixture	Mixture of Thin	$\theta K_0\left(\frac{r}{\rho_1}\right) + (1 - \theta)K_0\left(\frac{r}{\rho_2}\right)$	$\rho_1 = 3.20 \cdot 10^{-2}$ , $\rho_2 = 4.62$ , $\theta = 6.56 \cdot 10^{-1}$
Laplace mixture	Mixture of Thin	$\theta \exp\left(-\frac{r}{\rho_1}\right) + (1 - \theta) \exp\left(-\frac{r}{\rho_2}\right)$	$\rho_1 = 2.12 \cdot 10^{-2}$ , $\rho_2 = 3.91$ , $\theta = 6.18 \cdot 10^{-1}$
Gaussian mixture	Mixture of Thin	$\theta \exp\left(-\left(\frac{r}{\rho_1}\right)^2\right) + (1 - \theta) \exp\left(-\left(\frac{r}{\rho_2}\right)^2\right)$	$\rho_1 = 2.71 \cdot 10^{-2}$ , $\rho_2 = 1.03 \cdot 10^1$ , $\theta = 4.91 \cdot 10^{-1}$
WMY	Thin tail	$\left(\frac{r}{\rho}\right)^\kappa K_\kappa\left(\frac{r}{\rho}\right)$	$\rho = 2.26 \cdot 10^{-1}$ , $\kappa = 3.95 \cdot 10^{-9}$
Bessel	Thin tail	$K_0\left(\frac{r}{\rho}\right)$	$\rho = 2.15 \cdot 10^{-1}$
Laplace	Thin tail	$\exp\left(-\frac{r}{\rho}\right)$	$\rho = 2.15 \cdot 10^{-1}$
Gaussian	Thin tail	$\exp\left(-\left(\frac{r}{\rho}\right)^2\right)$	$\rho = 1.11$

There are several reasons for treating fat-tailed dispersal kernels as the default choice when modeling MPB. 1) Fat-tailed kernels provide a much better fit to the non-model dispersal kernel, computed with the minimum distance between parental and offspring infestations (Fig. 5). 2) Mixture models are less parsimonious, with  $\geq 3$  parameters. 3) According to the distance-stratified log likelihoods (Fig. 3), mixture-based kernels are better at predicting offspring infestations that are far away from any parental infestation. However, fat-tailed kernels are better at predicting nearby offspring infestations, which constitute the vast majority of new infestations.

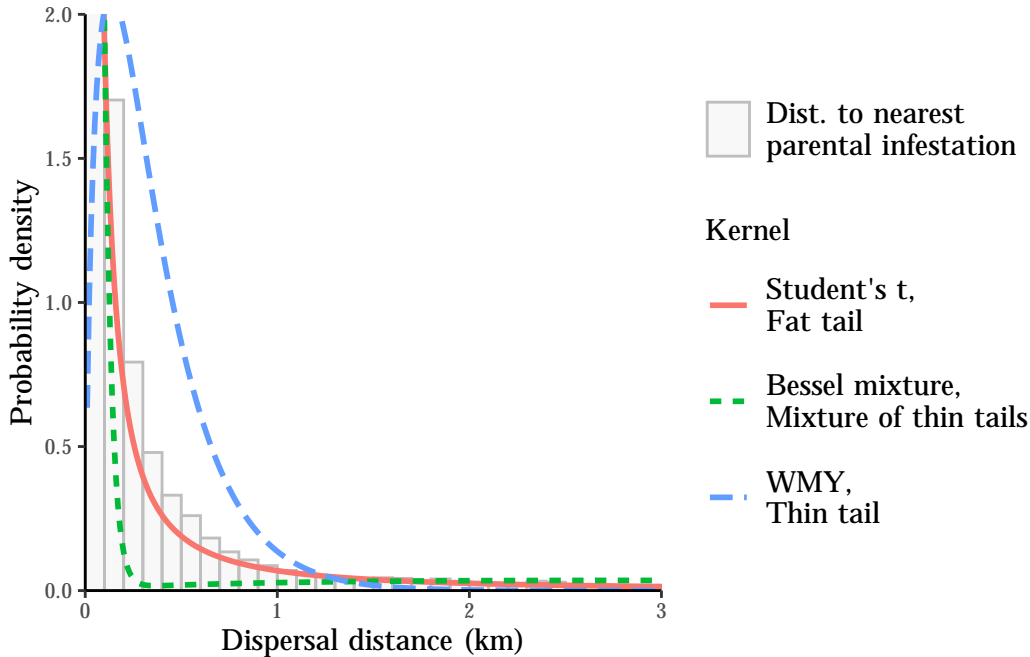


Figure 5: Predictions vs. observations for various dispersal kernels. The histogram gives the frequency of distances between infestations and the closest “parental infestation” from the previous year. The predictions come from the marginal dispersal kernels  $D_r(r)$ , i.e.,  $\int_0^{2\pi} D(r)r d\theta = 2\pi r D(r)$ , where  $r$  is the distance in kilometers,  $\theta$  is the angle in radians, and  $D(r)$  is the full density (see Table 2). For each class of distributional tail — thin, mixed, and fat — we display the model with the highest log likelihood.

## 4 Discussion

Fat-tailed dispersal kernels, particularly the Student’s  $t$ -distribution characterized by degrees of freedom  $\nu = 1.45$  and scale parameter  $\rho = 0.0118$ , emerge as the most effective way to model MPB dispersal. The Student’s  $t$  kernel yields dispersal distances with a median, mean, and 95<sup>th</sup> percentile of 0.080, 1.06, and 4.67 kilometers respectively. Unlike mixture-based dispersal kernels, the Student’s  $t$ -distribution faces no numerical model-fitting problems, only has 2 parameters, and successfully re-creates empirical patterns of distances between parental and offspring infestations (Fig. 5). Although such a simple model cannot hope to capture *all* aspects of MPB dispersal, the Student’s  $t$ -distribution serves as a useful first-order approximation for both researchers and conservation practitioners. Indeed, our stochastic simulations reveal that a simple fat-tailed dispersal kernel outperforms thin-tailed kernels in reconstructing the mountain pine beetle’s eastward expansion (Fig. 6).

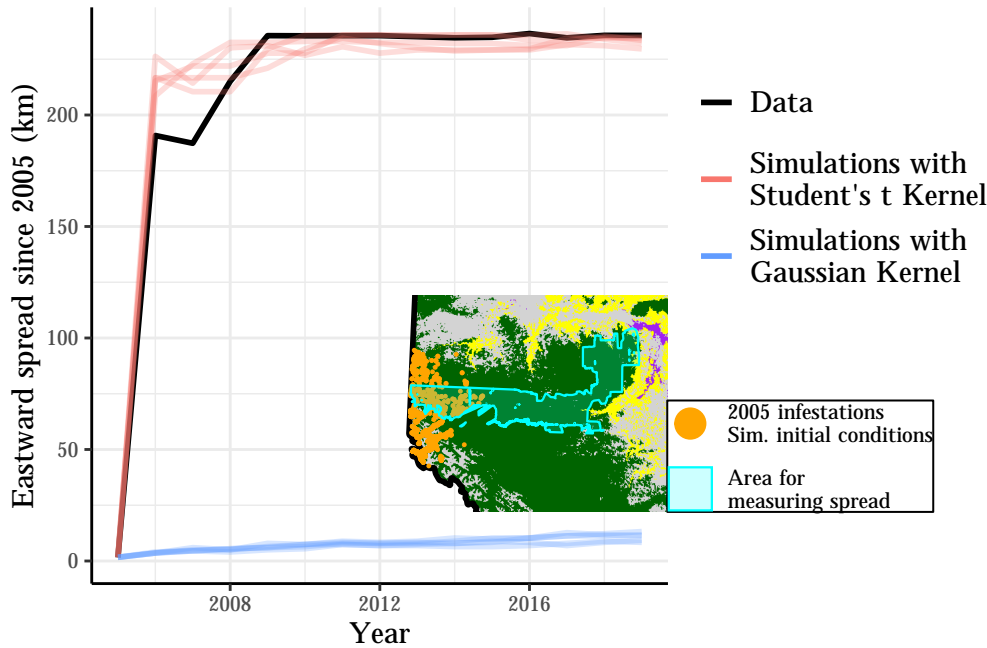


Figure 6: Fat-tailed redistribution kernels can explain the spread of MPB across Alberta. Using the 2005 infestations as the initial condition, we simulated the spatial spread of the MPB across the lodgepole pine zone of western Alberta (the dark green area in the inset plot). To summarize the spatial extent of infestations, we calculated the maximum easting coordinate for all infestations within the cyan polygon (see inset plot). This polygon is the intersection of Heli-GPS survey areas from 2005–2019.

The Student’s  $t$ -distribution has a clear interpretation in light of MPB biology: the Student’s  $t$ -distribution can be derived as an infinite mixture of Fickian diffusion processes with a gamma-distribution for stopping times or, equivalently, for the diffusion coefficients. It is this mixture that represents the variety of MPB dispersal strategies. Three types of dispersal behaviors roughly correspond to three classes of dispersal distances: Dispersal behaviors can be categorized into three types: short-range (typically  $\leq 100$  m), medium-range (up to 5 km), and long-range (above canopy, potentially up to 300 km). These distance ranges are approximate and illustrate orders of magnitude associated with each category. Short-range dispersal predominantly occurs under the canopy, with a large majority of beetles attracted to nearby plumes of aggregation pheromones (Safranyik et al., 1992; Robertson et al., 2007; Dodds and Ross, 2002). Medium-range dispersal involves a minority of beetles traveling up to 5 km to initiate pioneer attacks, resulting in semi-regular patterns of so-called spot infestations (Strohm et al., 2013). Proposed explanations for these pioneer attacks include evolutionary bet-hedging strategies (Raffa, 2001; Kautz et al., 2016) and the absence of guiding pheromones for early-emerging beetles. Long-range dispersal, observed in just 0–2.5% of beetles (Robertson et al., 2009; Safranyik et al., 1992), involves flight above the canopy, where beetles may be swept up by atmospheric winds and carried up to 300 km (Hiratsuka et al., 1982; Cerezke, 1989; Jackson et al., 2008). Fat-tailed dispersal kernels effectively interpolate between the three dispersal behaviors, thus capturing a wide range of dispersal distances.

Consistent with an inverse-gamma distribution of settling times, a recent flight-mill experiment shows that many beetles fly short distances, while few fly long distances (range 0–25 km; Evenden et al., 2014). The basis for this intraspecific variation is unclear. Larger beetles, which tend to emerge from larger trees (Graf et al., 2012), fly further on average. However, their flight distance is also more variable with different individuals flying short or long distances (Shegelski

et al., 2019). This polyphenism is thought to be an evolutionarily stable bet-hedging strategy (Kautz et al., 2016; Jones et al., 2020), where the short-distance dispersers are more likely to find host trees and conspecifics with which to perform mass attacks, and the risky longer-distance dispersers may enjoy the fitness advantages of arriving early to a large tree (Raffa, 2001 and sources therein).

Rare, long-distance “jackpot-dispersal” events, as described by the tails of fat-tailed dispersal kernels, are key for rapid spread. For example, in the case of MPB there is evidence that their range expansion across Alberta jumped eastward 250 km in a single year (Cooke and Carroll, 2017). These events can also yield a characteristic signature pattern of patchy spread on the landscape. Such patterns are most easily seen from Monte Carlo simulations of stochastic invasion processes that have a mixture of rare long- and common short-distance dispersal distances (Lewis and Pacala, 2000). The resulting spatial process, sometimes referred to as “stratified diffusion” Shigesada et al. (1995), exhibits a characteristic patchy pattern of spread, with rare long-distance dispersal events creating new invasion beachheads at a distance, followed by common short-distance dispersal coupled to growth dynamics generating growth of patches on a local scale. While a full mathematical analysis of such processes typically involves spatial moments of the associated point process of invasion (Lewis and Pacala, 2000), evidence of patchy spread in the spread of MPB can be seen visually from Figure 4.

The models we use are intentionally simple compared to the complex biology of MPB, but this simplicity is deliberate and serves a clear purpose. Beetle dispersal is influenced by many factors: at small spatial scales, it involves the phenology of beetle emergence, the production and diffusion of aggregation and anti-aggregation pheromones, forest micro-climates, and wind patterns (Amman and Logan, 1998; Biesinger et al., 2000); at larger spatial scales, dispersal involves temperature patterns, wind-storms, and the availability of host trees (Taylor et al., 2006a; Powell and Bentz, 2014). We contend that incorporating all these factors into the model is unnecessary and potentially counterproductive because 1) the specificity required for a detailed model would likely reduce its applicability to different areas or time periods, making it less useful for practitioners and scientists seeking to apply our results more broadly; and 2) a simple model with clear assumptions minimizes the risk of significant errors. In other words, we can be assured that dispersal distance estimates are not merely artifacts of model structure.

Previous research has provided a large range of dispersal estimates (recall Table 1). In particular, the work of Heavilin and Powell (2008) resulted in an implausibly small estimate of median dispersal distance: about 10 meters. This result can be attributed to a least-square model fitting procedure, which inadequately penalizes the prediction of zero new infestations in areas where infestations occur. Our model addresses these limitations by introducing a probabilistic landscape for new infestations, such that assigning a near-zero probability to an actual infestation incurs a near-infinite penalty. On the other side of the spectrum, the model of Koch et al. (2021) implies an implausibly large estimate of the median dispersal distance: about 17 km. This can be explained by the two-part structure of their model, which includes a dispersal sub-model and a pine susceptibility sub-model, where susceptibility is an increasing function of last year’s infestations. Therefore, the short distances between successive years’ infestations — normally attributed to short dispersal distance — are accounted for in the susceptibility sub-model, leaving the dispersal parameters relatively unconstrained. Our approach allows for a more accurate estimation of dispersal distances by focusing on the redistribution of infestations rather than individual beetles, and by taking into account inter-annual variation in beetle productivity through the predetermined number of new infestations.

The mathematical theory for spreading populations is based on models coupling dispersal and population growth dynamics; it generally assumes no significant Allee effect (i.e., positive density dependence) in the population growth dynamics (Lewis et al., 2016). We take this approach in our models despite MPB’s well-known Allee effect (Safranyik et al., 1975; Raffa and Berryman, 1983; Boone et al., 2011), which occurs because MPB must mass-attack trees



to deplete the trees' resin defenses. One justification is that MPB's Allee threshold — the population density at which per capita growth rates are negative — is small and varies with environmental conditions (Cooke et al., 2024). Another justification is that wind currents can carry large groups of beetles to the same destination, such that long-distance dispersal can be modeled as the movement of groups large enough to surpass the Allee threshold.

One advantage of using a dispersal kernel to model MPB is that it is relatively simple to understand and easily applied. The trade-off is that we do not capture all biological aspects of MPB dispersal. In particular, we do not include clustering mechanisms for dispersal — for long-distance dispersal it would be more accurate to assume beetles travel *en masse*, carried by wind currents — nor do we include clustering of beetles at small spatial scales to represent chemical signaling. This leads to a spatial distribution of simulated infestations that is unrealistically patchy (Fig. D.3). Additionally, our simulations (which generate Fig. 6) do not incorporate the effects of host tree depletion and assume pine density is constant, which is roughly true over short time scales but may not be true in heavily infested areas over entire outbreaks. Finally, beetles may disperse without necessarily infesting trees, potentially leading to underestimation of dispersal distances (as in Table 3). This bias arises from the Allee effect: beetles dispersing farther from infestation clusters have fewer companions for coordinating mass attacks, reducing their likelihood of successful attack and subsequent detection by Heli-GPS surveys. However, for reasons discussed in the previous paragraph (i.e., the clumped nature of dispersal and the apparent weakness of the Allee effect) we expect this bias to be minimal.

Our conclusions may also be particular to the study area or the years of study. We address these concerns about generalizability by considering an additional area 50 km east of the initial study area, as outlined in methods, and find qualitatively similar results (see Appendix A). We may additionally expect inter-annual variation in beetle dispersal given that dispersal distance may change with fluctuating environmental factors (Chen and Jackson, 2017; McCambridge, 1971; Powell and Bentz, 2014; Wijerathna and Evenden, 2020); but note that Carroll et al. (2017) find similar distances between years. We explored inter-annual variability by applying a Student's *t*-dispersal kernel to each year of data independently (Appendix B) though a comprehensive analysis remains beyond this paper's scope. The median dispersal distance fluctuates with a right-skewed distribution: most years show low distances (less than 100 meters), while a few years exhibit much larger distances (several hundred meters).

In conclusion, we find that relatively simple fat-tailed kernels can accurately characterize MPB dispersal. These kernels can describe both the short and long-distance dispersal modes of mountain pine beetle, which are both important at the landscape scale. In particular, the long-distance dispersal events captured by fat-tailed kernels are key for describing range expansion. We expect that this result applies for other species undergoing range expansions, and points to the importance of simple but accurate dispersal kernels for understanding and modeling these processes.

## 5 Acknowledgements

The authors would like to thank Xiaoqi Xie and K'evan Rastello for feedback. Funding for this research has been provided through grants to the TRIA-FoR Project to ML from Genome Canada (Project No. 18202) and the Government of Alberta through Genome Alberta (Grant No. L20TF), with contributions from the University of Alberta and fRI Research (Project No. U22004). This work was supported by Mitacs through the Mitacs Accelerate Program, in partnership with fRI Research. MB acknowledges the support of the Natural Sciences and Engineering Research Council of Canada (NSERC), [PDF – 568176 - 2022].

## 6 Author contributions

All authors conceived of the project; Evan C. Johnson performed the analysis; Evan C. Johnson and Micah Brush wrote the first draft; All authors contributed critically to the drafts and gave final approval for publication.

## 7 Data sources

Code and data will be made available on Zenodo ([TBD](#)).

## Appendix A Robustness check: Study area #2

The nature of MPB dispersal may vary across space, possibly due to un-modelled factors such as MPB population density, pine density, wind patterns, and annual temperature patterns. As reassurance that our dispersal models will produce reasonable results, even if applied outside of our focal study area, we re-ran our analysis in a second study area. This area is located approximately 50 km east of study area #1 (Fig. A.1) and has approximate dimensions of 50x50 km.

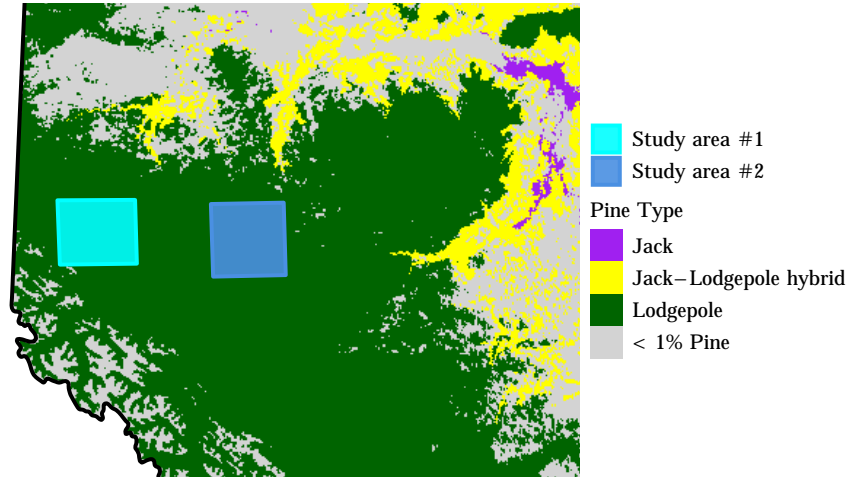


Figure A.1: The location and extent of both study areas in Alberta.

In study area #2, the estimated median and mean dispersal distances for the Student’s  $t$  kernel are 0.060 and 0.988 km respectively (Table A.1). These numbers are extremely similar to the estimates from study area #1 (Table 3). In study area #2, fat-tailed dispersal kernels are superior to mixture-based dispersal kernels with respect to the log likelihood; the true positive rate of predicting new infestations; and the correlation between log-scale predictions and infestations. For completeness, parameter estimates for study area #2 are provided in Table A.2.

Table A.1: Summary statistics of model fit and redistribution distances for the redistribution models, fit to data from study area #2. The abbreviation TPR stands for *True Positive Rate*;  $r$  is the correlation between the logarithm of the observed number of infestations and the logarithm of the expected number of infestations; and the last 4 columns refer to the distances between new infestations and their parental infestations.

Kernel name	Log likelihood	TPR	$r$ (log scale)	mean dist.	median dist.	75% dist.	95% dist.
Pareto	$-1.491 \cdot 10^6$	0.094	0.299	0.847	0.080	0.290	3.310
Student’s $t$	$-1.491 \cdot 10^6$	0.108	0.295	0.988	0.060	0.250	4.190
Bessel mixture	$-1.499 \cdot 10^6$	0.082	0.298	0.542	0.070	0.790	2.360
Laplace mixture	$-1.504 \cdot 10^6$	0.097	0.289	0.495	0.080	0.800	1.900
Gaussian mixture	$-1.518 \cdot 10^6$	0.106	0.274	0.710	0.500	1.260	2.170
WMY	$-1.582 \cdot 10^6$	0.000	0.241	0.307	0.250	0.420	0.780
Bessel	$-1.582 \cdot 10^6$	0.000	0.246	0.338	0.270	0.460	0.860
Laplace	$-1.605 \cdot 10^6$	0.000	0.231	0.350	0.290	0.470	0.830
Gaussian	$-1.657 \cdot 10^6$	0.000	0.194	0.652	0.610	0.870	1.270

Table A.2: Parameter values for the redistribution models, fit to data from study area #2. The parameters  $\rho$ ,  $\rho_1$ , and  $\rho_2$  have units of kilometers; the remaining parameters are dimensionless.

Kernel name	Tail type	$D(r) \propto$	Max likelihood estimate
Pareto	Fat-tail	$(r + \rho)^{-(1+\nu)}$	$\rho = 1.45 \cdot 10^{-2}$ , $\nu = 1.61$
Student's $t$	Fat-tail	$\left(1 + \frac{1}{\nu} \left(\frac{r}{\rho}\right)^2\right)^{-\frac{\nu+1}{2}}$	$\rho = 1.16 \cdot 10^{-2}$ , $\nu = 1.47$
Bessel mixture	Mixture of Thin	$\theta K_0\left(\frac{r}{\rho_1}\right) + (1 - \theta)K_0\left(\frac{r}{\rho_2}\right)$	$\rho_1 = 2.65 \cdot 10^{-2}$ , $\rho_2 = 7.84 \cdot 10^{-1}$ , $\theta = 5.90 \cdot 10^{-1}$
Laplace mixture	Mixture of Thin	$\theta \exp\left(-\frac{r}{\rho_1}\right) + (1 - \theta) \exp\left(-\frac{r}{\rho_2}\right)$	$\rho_1 = 1.55 \cdot 10^{-2}$ , $\rho_2 = 4.91 \cdot 10^{-1}$ , $\theta = 5.22 \cdot 10^{-1}$
Gaussian mixture	Mixture of Thin	$\theta \exp\left(-\left(\frac{r}{\rho_1}\right)^2\right) + (1 - \theta) \exp\left(-\left(\frac{r}{\rho_2}\right)^2\right)$	$\rho_1 = 2.23 \cdot 10^{-2}$ , $\rho_2 = 1.39$ , $\theta = 4.40 \cdot 10^{-1}$
WMY	Thin tail	$\left(\frac{r}{\rho}\right)^\kappa K_\kappa\left(\frac{r}{\rho}\right)$	$\rho = 1.95 \cdot 10^{-1}$ , $\kappa = 2.96 \cdot 10^{-8}$
Bessel	Thin tail	$K_0\left(\frac{r}{\rho}\right)$	$\rho = 2.15 \cdot 10^{-1}$
Laplace	Thin tail	$\exp\left(-\frac{r}{\rho}\right)$	$\rho = 1.75 \cdot 10^{-1}$
Gaussian	Thin tail	$\exp\left(-\left(\frac{r}{\rho}\right)^2\right)$	$\rho = 7.35 \cdot 10^{-1}$

## Appendix B Robustness check: inter-annual dispersal variability

Just as dispersal may exhibit spatial heterogeneity, it may also exhibit temporal heterogeneity. To examine this, we applied a Student's  $t$  dispersal kernel to each year's data independently. The resulting estimates reveal that the median dispersal distance fluctuates over time, although generally within narrow bounds. Specifically, while the median typically stays in the range of 0.02 – 0.1 km (centered around 0.05 km), there were 2/22 estimates which exceeded 0.3 km (Fig. B.1).

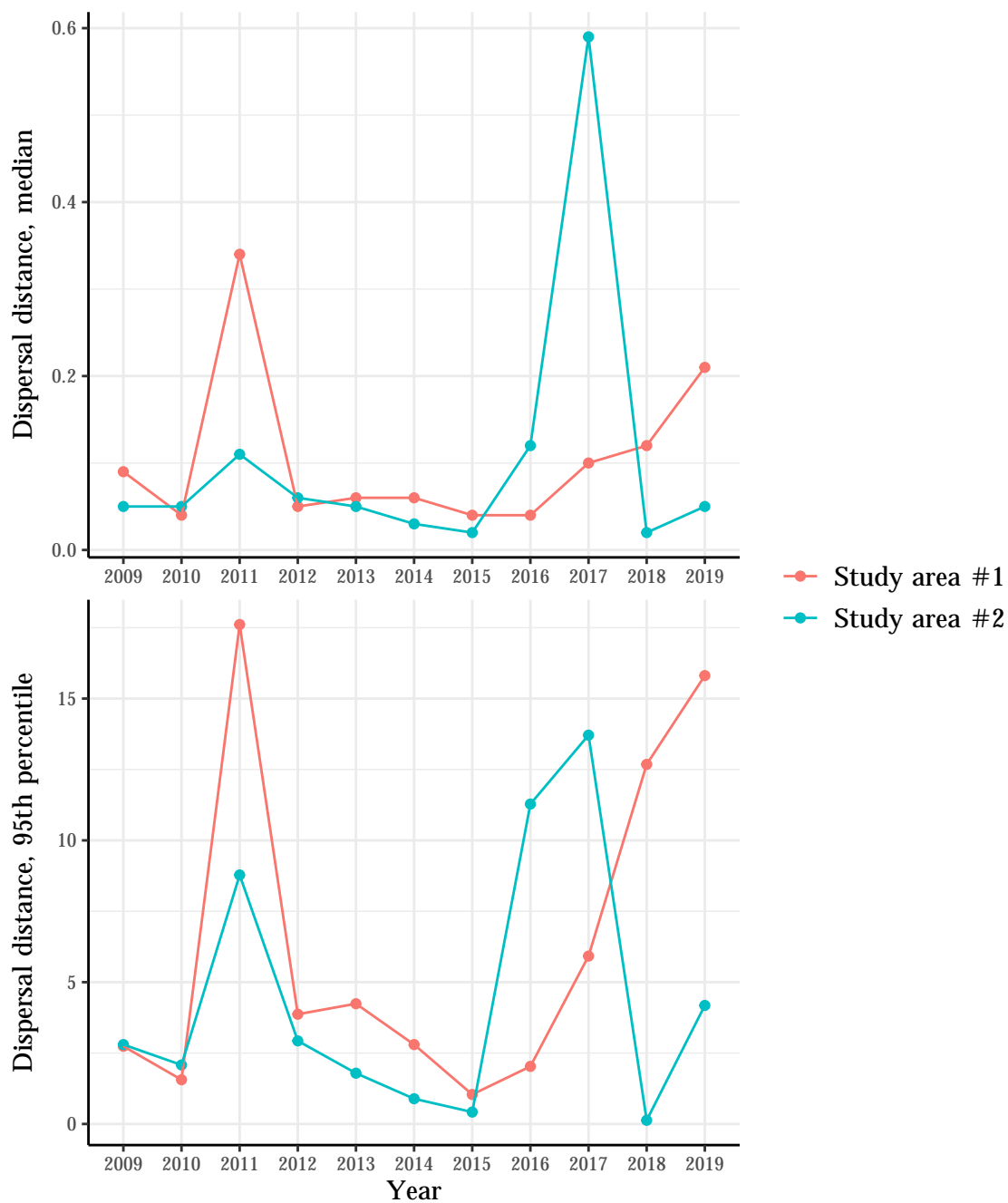


Figure B.1: Estimates of dispersal distance across years, for both study areas.

## Appendix C Additional information about characteristic length scales

Table 1 shows that the typical length scale of MPB dispersal varies widely across the literature, as well as data from related bark beetles. Here, in Table C.1, we show in more detail where we obtained the stated values in that table for MPB specifically, and in Table C.2 we show more detail for the stated values for related bark beetles.



Table C.1: Additional information on the stated values in Table 1 for mountain pine beetle. This includes information about the study location as well as more details on where we obtain the characteristic scale of infestation.

Study	Scale (m)	Study location	Source of scale
<a href="#">Aukema et al. (2008)</a>	18 000	British Columbia	Finds that the neighborhood of one cell is the most important predictor for infestations in 12 km x 12 km cells, which corresponds to roughly 18 km
<a href="#">Koch et al. (2021)</a>	17 000	British Columbia	Finds 17 km for the median dispersal distance from fitting an anisotropic WMY dispersal kernel to infestation data ( <i>personal communication</i> )
<a href="#">Preisler et al. (2012)</a>	10 000	Washington and Oregon	Finds that a distance weighted beetle pressure metric out to 10 km is one of the most important variables for all stages of outbreak
<a href="#">Sambaraju et al. (2012)</a>	6000	Western Canada	Finds that the most important variable in a statistical model is infestation in the previous year within the 12 km x 12 km cells
<a href="#">Howe et al. (2021)</a>	5000	British Columbia	Finds that a distance weighted beetle pressure metric from the previous year within 5 km provided the best explanatory power for a statistical model fit to infestation data
<a href="#">Carroll et al. (2017)</a>	2000	Alberta	Finds that more than 75% of new infestations occur within 2 km of “parent” polygons containing the infestations from the previous year using heli-GPS data
<a href="#">Simard et al. (2012)</a>	2000	Wyoming	Finds beetle pressure, up to 2 km, is the most important predictor for subsequent outbreaks for mountain pine beetle, spruce beetle, and Douglas-fir beetle
<a href="#">Robertson et al. (2009)</a>	1000	Canadian Rocky Mountains	Finds that most movements distances centre around 1 km using spatial-temporal analysis of moving polygons (STAMP)
<a href="#">Strohm et al. (2013)</a>	364	Sawtooth National Recreation Area, Idaho	Finds MPB attacks should be spaced by 364 m by studying pattern formation in a model of chemical signalling including diffusion and chemotaxis and parameterized with data from <a href="#">Biesinger et al. (2000)</a>
<a href="#">Powell and Bentz (2014)</a>	5 – 90	Sawtooth National Recreation Area, Idaho	Finds that density dependent motility varies from an unimpeded motility of 3.79 km <sup>2</sup> per day to 18.5 m <sup>2</sup> per day in a fully stocked stand by fitting a phenology and dispersal model to aerial detection data
<a href="#">Robertson et al. (2007)</a>	30 – 50	British Columbia	Finds that the most common distances between newly and previously attacked trees are 30 m and 50 m given a search radius of 100 m from previously attacked trees
<a href="#">Safranyik et al. (1992)</a>	30	British Columbia	Finds that 86% and 93% of total captured beetles were found within 30 m of release site in a mark-recapture experiment in two years
<a href="#">Heavilin and Powell (2008)</a>	10 – 15	Sawtooth National Recreation Area, Idaho	Finds a mean and median dispersal distance of between 10 m to 15 m by fitting Gaussian and exponential dispersal kernels to aerial detection data
<a href="#">Goodsman et al. (2016)</a>	10	British Columbia and Alberta	Finds a median dispersal distance of 10 m by parameterizing a 2D dispersal kernel with mark-recapture data from <a href="#">Safranyik et al. (1992)</a>



Table C.2: Additional information on the stated values in Table 1 for related bark beetles. This includes information about the study location as well as more details on where we obtain the characteristic scale of infestation.

Study	Scale (m)	Study location	Bark beetle species	Source of scale
<a href="#">Withrow et al. (2013)</a>	1000 – 2500	Colorado and Wyoming	Douglas-fir beetle	Finds average standard dispersal distances — distances at which 68% of infestations dispersed in a given year — between 1000 m and 2500 m by quantifying the distance between infestations and modeling these distances using a cumulative Gaussian function
<a href="#">Turchin and Thoeny (1993)</a>	690	Louisiana	Southern pine beetle	Finds a median dispersal distance of 690 m for released beetles by fitting a dispersal model with mark-recapture data
<a href="#">Werner and Holsten (1997)</a>	90 – 300	Alaska	Spruce beetle	Finds that most recaptured beetles from standing trees dispersed between 90 m and 300 m in mark-recapture experiments
<a href="#">Zumr (1992)</a>	200	Southern Bohemia	European spruce beetle	Finds that most beetles (about 70%) were captured within 200 m of release in mark-recapture experiments
<a href="#">Dodds and Ross (2002)</a>	200	Idaho	Douglas-fir beetle	Finds that most beetles (over 90%) were captured within 200 m of release in mark-recapture experiments
<a href="#">Kautz et al. (2011)</a>	100	Bavaria	European spruce beetle	Finds that 65% of new infestations occurred within 100 m of the previous year's infestations
<a href="#">Zolubas and Byers (1995)</a>	10	Western Lithuania	European spruce beetle	Finds that most beetles (about 67%) were captured within 10 m of release in mark-recapture experiments for the second flight

## Appendix D Additional figures & tables

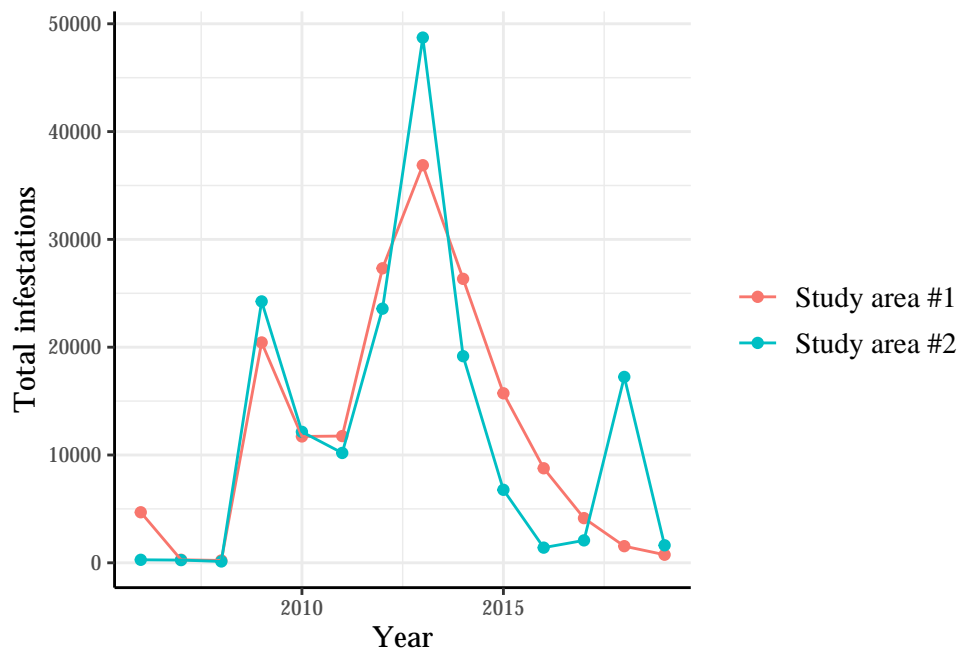


Figure D.1: Time series of total infestations in both study areas. A large number of beetles were present from 2009–2019.

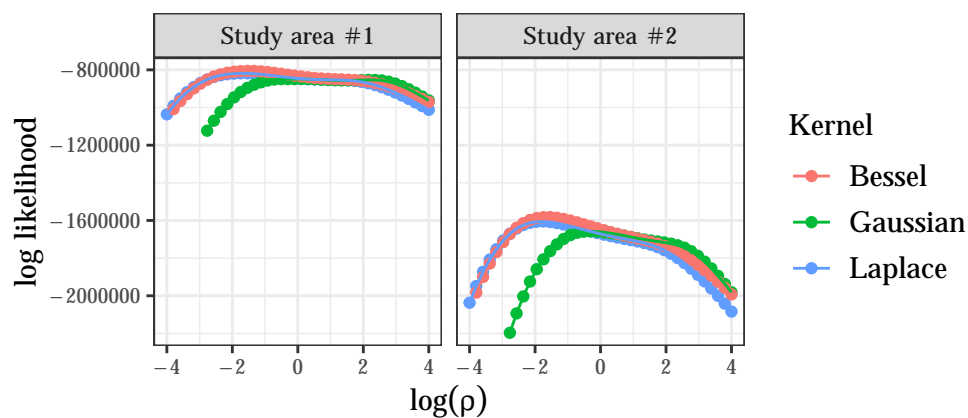


Figure D.2: Likelihood profiles for the three one-parameter redistribution models. The gradient of the log likelihood is relatively flat for large values of the scale parameter  $\rho$ , which can cause the failure of gradient-based optimization methods. Instead, we used the grid search method to find the Maximum Likelihood Estimates for these models.

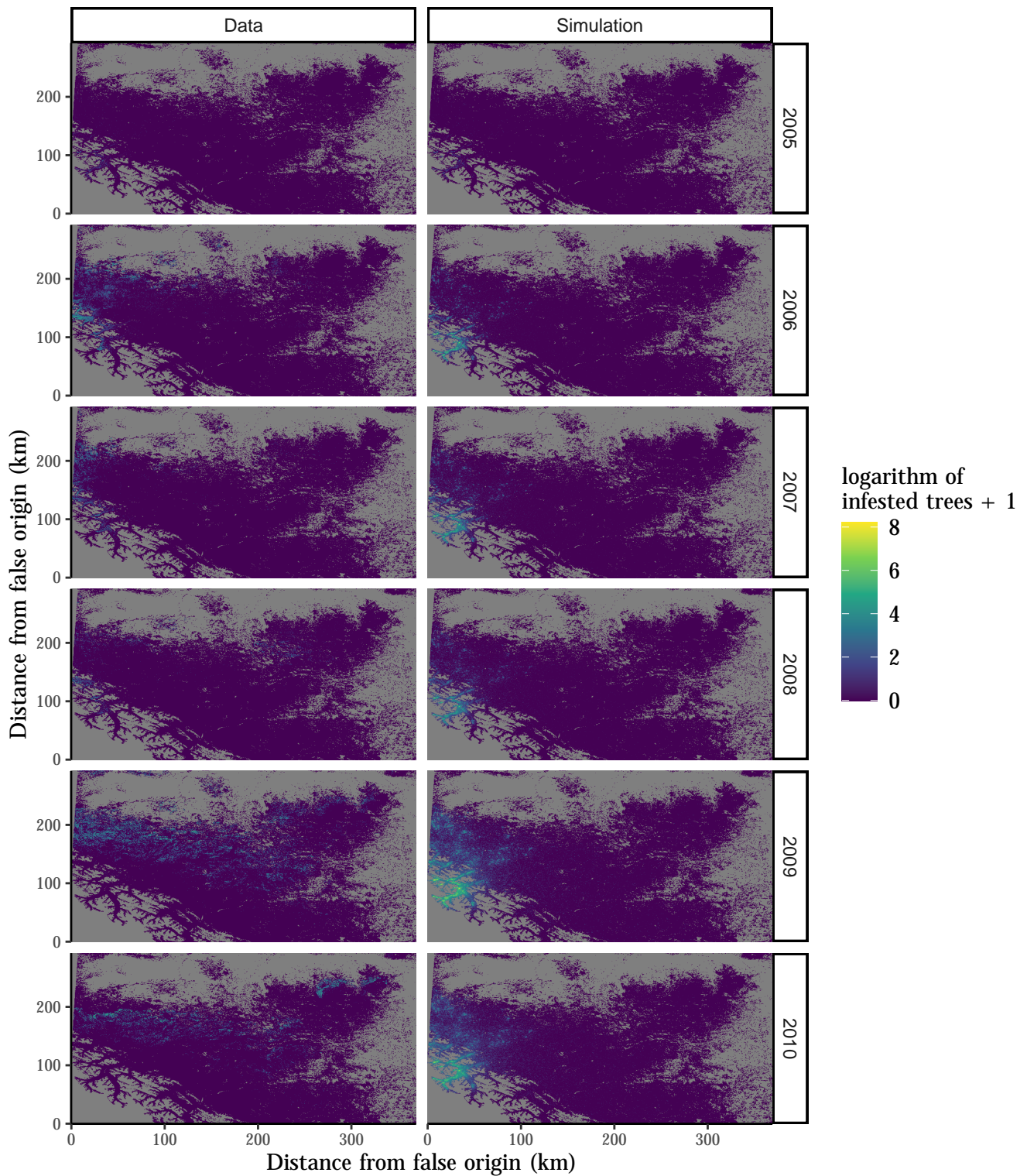


Figure D.3: Comparison of the spatial distribution of infestations for both real and simulated data. Our simulations do not account for resource depletion, which leads to an unrealistic concentration of future infestations around the initial infestations. Our simulations do not account for beetle aggregation or clumpy dispersal, which leads to an unrealistically high spatial dispersion of infestations.

## References

- Amman, G. D. and Logan, J. A. (1998). Silvicultural control of mountain pine beetle: Prescriptions and the influence of microclimate. *American Entomologist*, 44(3):166–178.
- Aukema, B. H., Carroll, A. L., Zheng, Y., Zhu, J., Raffa, K. F., Dan Moore, R., Stahl, K., and Taylor, S. W. (2008). Movement of outbreak populations of mountain pine beetle: influences of spatiotemporal patterns and climate. *Ecography*, 31(3):348–358.
- Beaudoin, A., Bernier, P., Guindon, L., Villemaire, P., Guo, X., Stinson, G., Bergeron, T., Magnussen, S., and Hall, R. (2014). Mapping attributes of canada’s forests at moderate resolution through k nn and modis imagery. *Canadian Journal of Forest Research*, 44(5):521–532.
- Benhamou, S. (2007). How Many Animals Really Do the Lévy Walk? *Ecology*, 88(8):1962–1969.
- Biesinger, Z., Powell, J., Bentz, B., and Logan, J. A. (2000). Direct and indirect parametrization of a localized model for the mountain pine beetle — lodgepole pine system. *Ecological Modelling*, 129(2):273–296.
- Bleiker, K. P., editor (2019). *Risk assessment of the threat of mountain pine beetle to Canada’s boreal and eastern pine forests : prepared for the Canadian Council of Forest Ministers, Forest Pest Working Group*. Canadian Council of Forest Ministers.
- Bleiker, K. P., O’Brien, M. R., Smith, G. D., and Carroll, A. L. (2014). Characterisation of attacks made by the mountain pine beetle (coleoptera: Curculionidae) during its endemic population phase. *The Canadian Entomologist*, 146(3):271–284.
- Boone, C. K., Aukema, B. H., Bohlmann, J., Carroll, A. L., and Raffa, K. F. (2011). Efficacy of tree defense physiology varies with bark beetle population density: a basis for positive feedback in eruptive species. *Canadian Journal of Forest Research*, 41(6):1174–1188.
- Broadbent, S. R. and Kendall, D. G. (1953). The Random Walk of *Trichostromylytus retortaeformis*. *Biometrics*, 9(4):460.
- Carroll, A., Régnière, J., Logan, J., Taylor, S., Bentz, B., and Powell, J. (2006a). Impacts of climate change on range expansion by the mountain pine beetle. Technical report, Pacific Forestry Centre Canada.
- Carroll, A., Seely, B., Welham, C., and Nelson, H. (2017). Assessing the effectiveness of alberta’s forest management program against the mountain pine beetle: Final report for fri research project 246.18 parts 1 and 2. Technical report, FRI Research.
- Carroll, A. L., Aukema, B., Raffa, K., Linton, D., Smith, G. D., and Lindgren, B. (2006b). Mountain pine beetle outbreak development: the endemic—incipient epidemic transition. Mpci project # 1.03, Natural Resources Canada, Canadian Forest Service.
- Carroll, A. L., Safranyik, L., et al. (2003). The bionomics of the mountain pine beetle in lodgepole pine forests: establishing a context. In *Mountain pine beetle symposium: Challenges and solutions*, pages 21–32. Natural Resources Canada, Canadian Forest Service.
- Cerezke, H. F. (1989). Mountain Pine Beetle Aggregation Semiochemical Use in Alberta and Saskatchewan, 1983–1987. General Technical Report INT-262, United States Department of Agriculture, Forest Service, Ogden, Utah, Kalispell, Montana.

- Chen, H. and Jackson, P. L. (2017). Climatic conditions for emergence and flight of mountain pine beetle: implications for long-distance dispersal. *Canadian Journal of Forest Research*, 47(7):974–984.
- Cooke, B., MacQuarrie, C., and Carroll, A. (2024). On the deduction and quantification of irruptive dynamics in mountain pine beetle population and proxy data. *Journal of Applied Entomology*.
- Cooke, B. J. and Carroll, A. L. (2017). Predicting the risk of mountain pine beetle spread to eastern pine forests: Considering uncertainty in uncertain times. *Forest Ecology and Management*, 396:11–25.
- Corbett, L. J., Withey, P., Lantz, V., and Ochuodho, T. (2016). The economic impact of the mountain pine beetle infestation in british columbia: provincial estimates from a cge analysis. *Forestry: An International Journal of Forest Research*, 89(1):100–105.
- Creeden, E. P., Hicke, J. A., and Buotte, P. C. (2014). Climate, weather, and recent mountain pine beetle outbreaks in the western united states. *Forest Ecology and Management*, 312:239–251.
- Cudmore, T. J., Björklund, N., Carroll, A. L., and Lindgren, S. B. (2010). Climate change and range expansion of an aggressive bark beetle: evidence of higher beetle reproduction in naïve host tree populations. *Journal of Applied Ecology*, 47(5):1036–1043.
- Cullingham, C. I., James, P. M., Cooke, J. E., and Coltman, D. W. (2012). Characterizing the physical and genetic structure of the lodgepole pine × jack pine hybrid zone: mosaic structure and differential introgression. *Evolutionary applications*, 5(8):879–891.
- Dodds, K. J. and Ross, D. W. (2002). Sampling range and range of attraction of *Dendroctonus pseudotsugae* pheromone-baited traps. *The Canadian Entomologist*, 134(3):343–355.
- Evenden, M. L., Whitehouse, C. M., and Sykes, J. (2014). Factors Influencing Flight Capacity of the Mountain Pine Beetle (Coleoptera: Curculionidae: Scolytinae). *Environmental Entomology*, 43(1):187–196.
- Goodsman, D. W., Koch, D., Whitehouse, C., Evenden, M. L., Cooke, B. J., and Lewis, M. A. (2016). Aggregation and a strong Allee effect in a cooperative outbreak insect. *Ecological Applications*, 26(8):2623–2636.
- Government of Alberta (2016). Mountain pine beetle detection and management in alberta. Technical report, Government of Alberta, Agriculture and Forestry. Accessed: 2024-09-05.
- Graf, M., Reid, M., Aukema, B., and Lindgren, B. (2012). Association of tree diameter with body size and lipid content of mountain pine beetles. *The Canadian Entomologist*, 144(3):467–477.
- Heavilin, J. and Powell, J. A. (2008). A novel method of fitting spatio-temporal models to data, with applications to the dynamics of mountain pine beetles. *Natural Resource Modeling*, 21(4):489–524.
- Hiratsuka, Y., Cerezke, H. F., Moody, B. H., Petty, J. A., and Still, G. N. (1982). Forest insect and disease conditions in Alberta, Saskatchewan, Manitoba, and the Northwest Territories in 1981 and predictions for 1982. Information report NOR-X-239, Environment Canada, Canadian Forestry Service, Northern Forest Research Centre, Edmonton, Alberta.

- Howe, M., Carroll, A., Gratton, C., and Raffa, K. F. (2021). Climate-induced outbreaks in high-elevation pines are driven primarily by immigration of bark beetles from historical hosts. *Global Change Biology*, 27(22):5786–5805.
- Jackson, P. L., Straussfogel, D., Lindgren, B. S., Mitchell, S., and Murphy, B. (2008). Radar observation and aerial capture of mountain pine beetle, *Dendroctonus ponderosae* Hopk. (Coleoptera: Scolytidae) in flight above the forest canopy. *Canadian Journal of Forest Research*, 38(8):2313–2327.
- Jones, K. L., Rajabzadeh, R., Ishangulyyeva, G., Erbilgin, N., and Evenden, M. L. (2020). Mechanisms and consequences of flight polyphenisms in an outbreaking bark beetle species. *Journal of Experimental Biology*, 223(12):jeb219642.
- Jones, K. L., Shegelski, V. A., Marculis, N. G., Wijerathna, A. N., and Evenden, M. L. (2019). Factors influencing dispersal by flight in bark beetles (Coleoptera: Curculionidae: Scolytinae): from genes to landscapes. *Canadian Journal of Forest Research*, 49(9):1024–1041.
- Joseph, J. and Sendner, H. (1958). Über die horizontale Diffusion im Meere. *Deutsche Hydrografische Zeitschrift*, 11(2):49–77.
- Kautz, M., Dworschak, K., Gruppe, A., and Schopf, R. (2011). Quantifying spatio-temporal dispersion of bark beetle infestations in epidemic and non-epidemic conditions. *Forest Ecology and Management*, 262(4):598–608.
- Kautz, M., Imron, M. A., Dworschak, K., and Schopf, R. (2016). Dispersal variability and associated population-level consequences in tree-killing bark beetles. *Movement Ecology*, 4(1):9.
- Koch, D., Lewis, M. A., and Lele, S. (2021). The Signature of Endemic Populations in the Spread of Mountain Pine Beetle Outbreaks. *Bulletin of Mathematical Biology*, 83(6):65.
- Koch, D. C., Lewis, M. A., and Lele, S. R. (2020). A unifying theory for two-dimensional spatial redistribution kernels with applications in population spread modelling. *Journal of The Royal Society Interface*, 17(170):20200434.
- Kot, M., Lewis, M. A., and van den Driessche, P. (1996). Dispersal Data and the Spread of Invading Organisms. *Ecology*, 77(7):2027–2042.
- Lewis, M. A. and Pacala, S. (2000). Modeling and analysis of stochastic invasion processes. *Journal of mathematical biology*, 41:387–429.
- Lewis, M. A., Petrovskii, S., and Potts, J. (2016). *The mathematics behind biological invasions*. Springer Berlin Heidelberg, New York, NY.
- Liu, B. R. and Kot, M. (2019). Accelerating invasions and the asymptotics of fat-tailed dispersal. *Journal of theoretical biology*, 471:22–41.
- McCambridge, W. F. (1971). Temperature Limits of Flight of the Mountain Pine Beetle, *Dendroctonus ponderosae*1. *Annals of the Entomological Society of America*, 64(2):534–535.
- Nealis, V. G. and Cooke, B. J. (2014). Risk assessment of the threat of mountain pine beetle to canada’s boreal and eastern pine forests. Technical report, Natural Resources Canada, Canadian Forest Service, Pacific Forestry Centre.
- News, C. (2023). Mountain pine beetle populations down by 94 per cent in alberta since 2019: Province. Accessed: 2024-09-03.

- Powell, J. A. and Bentz, B. J. (2014). Phenology and density-dependent dispersal predict patterns of mountain pine beetle (*Dendroctonus ponderosae*) impact. *Ecological Modelling*, 273:173–185.
- Preisler, H. K., Hicke, J. A., Ager, A. A., and Hayes, J. L. (2012). Climate and weather influences on spatial temporal patterns of mountain pine beetle populations in Washington and Oregon. *Ecology*, 93(11):2421–2434.
- Raffa, K. F. (2001). Mixed messages across multiple trophic levels: the ecology of bark beetle chemical communication systems. *Chemoecology*, 11(2):49–65.
- Raffa, K. F. and Berryman, A. A. (1983). The Role of Host Plant Resistance in the Colonization Behavior and Ecology of Bark Beetles (Coleoptera: Scolytidae). *Ecological Monographs*, 53(1):27–49.
- Robertson, C., Nelson, T. A., and Boots, B. (2007). Mountain Pine Beetle Dispersal: The Spatial–Temporal Interaction of Infestations. *Forest Science*, 53(3):395–405.
- Robertson, C., Nelson, T. A., Jelinski, D. E., Wulder, M. A., and Boots, B. (2009). Spatial–temporal analysis of species range expansion: the case of the mountain pine beetle, *Dendroctonus ponderosae*. *Journal of Biogeography*, 36(8):1446–1458.
- Safranyik, L. and Carroll, A. L. (2006). The biology and epidemiology of the mountain pine beetle in lodgepole pine forests. In Safranyik, L. and Wilson, B., editors, *The mountain pine beetle: A synthesis of biology, management, and impacts on lodgepole pine*, pages 3–66. Natural Resources Canada, Canadian Forest Service, Pacific Forestry Centre, Victoria, British Columbia.
- Safranyik, L., Linton, D. A., Silversides, R., and McMullen, L. H. (1992). Dispersal of released mountain pine beetles under the canopy of a mature lodgepole pine stand. *Journal of Applied Entomology*, 113(1-5):441–450.
- Safranyik, L., Shrimpton, D., Whitney, H., et al. (1975). An interpretation of the interaction between lodgepole pine, the mountain pine beetle and its associated blue stain fungi in western Canada. *Management of lodgepole pine ecosystems*, 1:406–428.
- Sambaraju, K. R., Carroll, A. L., Zhu, J., Stahl, K., Moore, R. D., and Aukema, B. H. (2012). Climate change could alter the distribution of mountain pine beetle outbreaks in western Canada. *Ecography*, 35(3):211–223.
- Shegelski, V. A., Evenden, M. L., and Sperling, F. A. H. (2019). Morphological variation associated with dispersal capacity in a tree-killing bark beetle *Dendroctonus ponderosae* Hopkins. *Agricultural and Forest Entomology*, 21(1):79–87.
- Shigesada, N., Kawasaki, K., and Takeda, Y. (1995). Modeling Stratified Diffusion in Biological Invasions. *The American Naturalist*, 146(2):229–251.
- Simard, M., Powell, E. N., Raffa, K. F., and Turner, M. G. (2012). What explains landscape patterns of tree mortality caused by bark beetle outbreaks in Greater Yellowstone? *Global Ecology and Biogeography*, 21(5):556–567.
- Six, D. L., Vergobbi, C., and Cutter, M. (2018). Are Survivors Different? Genetic-Based Selection of Trees by Mountain Pine Beetle During a Climate Change-Driven Outbreak in a High-Elevation Pine Forest. *Frontiers in Plant Science*, 9.
- Skellam, J. G. (1951). Random Dispersal in Theoretical Populations. *Biometrika*, 38(1/2):196.

- Srivastava, V. and Carroll, A. L. (2023). Dynamic distribution modelling using a native invasive species, the mountain pine beetle. *Ecological Modelling*, 482:110409.
- Strohm, S., Tyson, R. C., and Powell, J. A. (2013). Pattern Formation in a Model for Mountain Pine Beetle Dispersal: Linking Model Predictions to Data. *Bulletin of Mathematical Biology*, 75(10):1778–1797.
- Taylor, S. W., Carroll, A. L., Alfaro, R. I., and Safranyik, L. (2006a). Forest, Climate and Mountain Pine Beetle Outbreak Dynamics in Western Canada. In Safranyik, L. and Wilson, B., editors, *The mountain pine beetle: A synthesis of biology, management, and impacts on lodgepole pine*. Natural Resources Canada, Canadian Forest Service, Pacific Forestry Centre, Victoria, British Columbia.
- Taylor, S. W., Carroll, A. L., Alfaro, R. I., Safranyik, L., et al. (2006b). Forest, climate and mountain pine beetle outbreak dynamics in western canada. In Safranyik, L. and Wilson, B., editors, *Detection, mapping, and monitoring of the mountain pine beetle*, pages 67–94. Natural Resources Canada, Canadian Forest Service, Pacific Forestry Centre.
- Team, R. C. (2022). R: A Language and Environment for Statistical Computing.
- Turchin, P. and Thoeny, W. T. (1993). Quantifying Dispersal of Southern Pine Beetles with Mark-Recapture Experiments and a Diffusion Model. *Ecological Applications*, 3(1):187–198.
- Walton, A. (2012). Provincial-level projection of the current mountain pine beetle outbreak: Update of the infestation projection based on the provincial aerial overview surveys of forest health conducted from 1999 through 2011 and the bcmpb model (year 9). Technical report, BC Forest Service.
- Werner, R. A. and Holsten, E. H. (1997). Dispersal of the Spruce Beetle, *Dendroctonus rufipennis*, and the Engraver Beetle, *Ips perturbatus*, in Alaska. Research Paper PNW-RP-501, U.S. Department of Agriculture, Forest Service, Pacific Northwest Research Station, Portland, OR.
- Wijerathna, A. and Evenden, M. (2020). Effect of Environmental Conditions on Flight Capacity in Mountain Pine Beetle (Coleoptera: Curculionidae: Scolytinae). *Journal of Insect Behavior*, 33(5):201–215.
- Withrow, J. R., Lundquist, J. E., and Negrón, J. F. (2013). Spatial Dispersal of Douglas-Fir Beetle Populations in Colorado and Wyoming. *ISRN Forestry*, 2013:1–10.
- Zolubas, P. and Byers, J. A. (1995). Recapture of dispersing bark beetle *Ips typographus* L. (Col., Scolytidae) in pheromone-baited traps: regression models. *Journal of Applied Entomology*, 119(1-5):285–289.
- Zumr, V. (1992). Dispersal of the spruce bark beetle *Ips typographus* (L.) (Col., Scolytidae) in spruce woods1. *Journal of Applied Entomology*, 114(1-5):348–352.